

Impact of Variable Magnetic Field and Convective Boundary Condition on a Stretched 3D Radiative Flow of Cu-H₂O Nanofluid

*M.K. Nayak, **Sachin Shaw, ***Ali J. Chamkha

*Department of Physics, Radhakrishna Institute of Technology and Engineering, Biju Patnaik University of Technology, Odisha, India (mkn2122@gmail.com)

**Department of Mathematics and Statistical Sciences, Botswana International University of Science and Technology, Private Bag 16, Palapye, Botswana

***Department of Mechanical Engineering, Prince Mohammad Bin Fahd University, Al-Khobar 31952, Saudi Arabia

Abstract

The present study is dealt with the influence of a variable magnetic field and thermal radiation on three-dimensional flow of incompressible nanofluid over an exponentially-stretching sheet in association with a convective boundary condition. Patel model is employed in this study because this model contributes more thermal conductivity and hence the heat transfer capability of nanofluids compared to the Maxwell and Brinkman model. In the present analysis, base fluids such as water, 30% ethylene glycol, 50% ethylene glycol and nanoparticles such as Cu, Ag and Al₂O₃ are considered. The transformed governing differential equations are solved using fourth-order Runge-Kutta method along with shooting technique and secant method is employed for better approximation. The significant impact of the variable magnetic field and the thermal radiation on the dimensionless velocity, temperature, skin friction and the Nusselt number has been analyzed. The important outcome of the present study is that the Lorentz force due to the presence of the magnetic field impinges its resistance on the fluid motion leading to diminution of the wall shear stresses(axial as well as transverse) in association with a thinner momentum boundary layer and reduction in the heat transfer rate from the sheet developing thicker thermal boundary layer.

Key words

MHD, 3D flow, Nanofluid, Exponential stretching sheet, Convective boundary condition, Thermal radiation.

1. Introduction

In the last few decades, in the light of massive growing of inevitable significant engineering applications of nanofluids in emerging diversified fields such as better coolant in computers and safer coolant in nuclear reactors, cancer therapy, heat exchangers, micro-channel heat sinks and several electronic devices for use in military sectors, vehicles and transformers, the waste heat removal equipment design, manufacturing of materials and chemicals, oil and gas, paper and printing, polymer extrusion, glass blowing, rapid spray cooling, cooling of microelectronics, wire drawing and quenching in metal foundries and as refrigerant/lubricant mixtures enabling to chill or cool buildings have motivated and encouraged numerous researchers to investigate the several aspects of flow and heat transfer of nanofluids over various types of surfaces.

Indeed, nanofluids are fluids that possess nanoparticles viz. metals, oxides, carbides, nitrides and carbon nanotubes (particles of 100nm or less size) along with many conventional fluids (base fluids) such as water, kerosene, engine oil, toluene, ethylene glycol and tri-ethylene glycol etc. Use of additive is a relevant process that enhances the heat transfer capabilities of base fluids appreciably. Because of higher thermal conductivity of nanofluids, these are served as best suitable coolants in the above mentioned applications. There is a need to look at history not only from the discovery of behavior of nanofluids over stretching surface, but also from the discovery of flow and heat transfer over stretching surfaces. Choi [1] discovered first to the enhancement of thermal conductivity of nanofluids. The contribution of Khan and Pop [2] to investigate the boundary layer flow of nanofluids over stretching surfaces can never be sidelined. Later on, Makinde and Aziz [3] implemented the convective boundary condition in exhibiting boundary-layer flow of a nanofluid over a stretching surface. Now other researchers [4-10] have been working towards roping in the investigation for further development in this area.

It has to be accepted that the vital and inevitable applications of MHD nanofluid flow and heat transfer include wound treatment, sterilized equipments, gastric medications, targeted drug release, asthma treatment, cancer therapy, magnetic cell separation, magnetic resonance imaging, hyperthermia for tumor extraction etc. By dint of such significant applications many researchers have been motivated to study in the related areas. Sheikholeslami et al. [11] explored the effect of magnetic field in the flow and heat transfer of nanofluid in a rotating system. Ismael et al. [12]

discussed the impact of inclined magnetic field associated with partial slip and constant heat flux undergoing mixed convection in a cavity with a nanofluid. Furthermore, 3 hermos-physical properties of water based nanofluids past an exponential stretching sheet were explored by Nadeem et al. [13]. Moreover, Hayat et al. [14] studied MHD peristaltic flow of hyperbolic tangent nanofluid associated with slip and Joule heating in an inclined channel. In their study, they noticed that larger values of Hartman number enhance the temperature in response to Joule heating effect. We prefer to highlight here that Makinde and Animasaun [15] studied a wonderful job regarding MHD nanofluid flow with bio-convection over an upper surface of a paraboloid of revolution. They found that at fixed magnetic parameter, the local skin friction becomes more at large thickness parameter whereas local heat transfer rate becomes less at small temperature parameter.

In fact, convective boundary condition represents the heat transfer rate through the surface which is proportional to the local difference in temperature with ambient conditions. In other words, convective boundary condition enhances the temperature and therefore the thermal conductivity of the nanofluids. This is why it is very important to consider the convective boundary condition as more suitable model compared to isothermal conditions. Aziz [16] employed successfully the convective boundary condition in radiative flow over a flat plate. Nayak [17] discussed the effect of convective boundary conditions in a radiating nanofluid flow over a shrinking sheet subject to viscous dissipation. Furthermore, Nayak et al. [18] analysed the influence of convective boundary condition on heat transfer over a exponential surface.

It is obvious by the fact that thermal radiation effect is felt to be important in the situations with large temperature gap between the boundary surface and ambient fluid. Also such effect is used to obtain high thermal efficiency from devices operating at high temperature levels for space applications. That is why the radiation effects are essentially used in the design of many advanced conversion systems. Makinde and Ogulu [19] found by investigation that increase in thermal radiation enhances the non-dimensional temperature profiles in a flow of a variable viscosity fluid over a vertical porous plate in presence of transverse magnetic field. Nayak [20] analyzed in his study that thermal radiation should be kept minimum so as to achieve more cooling due to MHD viscoelastic fluid flow over a stretching sheet. The effect of thermal radiation as well as viscous dissipation in response to chemical reaction was reported by Mabood et al. [21]. In their investigation it is described that thermal radiation significantly influences the temperature distributions of nanofluids in the manner that thermal radiation increases the thermal diffusion thereby increasing the fluid temperature irrespective of nature of nanoparticles.

The above literature studies divulges that no one has discussed so far the impact of a transverse variable magnetic field and thermal radiation on three-dimensional nanofluid flow past an exponentially-stretching sheet with a convective boundary condition employing Patel model [22]. Hence, we are motivated to investigate the impact of variable magnetic field and thermal radiation in 3D nanofluid flows over an exponentially-stretching sheet using a convective boundary condition. In the presented sections, the similarity transformed governing boundary layer equations are solved numerically using the fourth-order Runge-Kutta method along with the shooting technique. The influence of the dimensionless velocity and temperature along with the skin friction and the local Nusselt number are well discussed and presented in the form of literature, graphs and tables.

2. Formulation of the Problem

We consider a steady three-dimensional boundary layer flow of an electrically-conducting magnetohydrodynamic nanofluid over an exponentially-stretching sheet as shown in Fig.1. Assume that (1) the flow is steady, laminar and incompressible (2) the thermal conductivity and specific heat are temperature independent, (3) gravitational effect is negligible, (4) convective boundary condition representing heat transfer rate through the surface is introduced, (5) a variable magnetic field $B = B_0 e^{\frac{x+y}{2L}}$ is introduced in the flow, and (6) the induced magnetic field and the electric field are negligible.

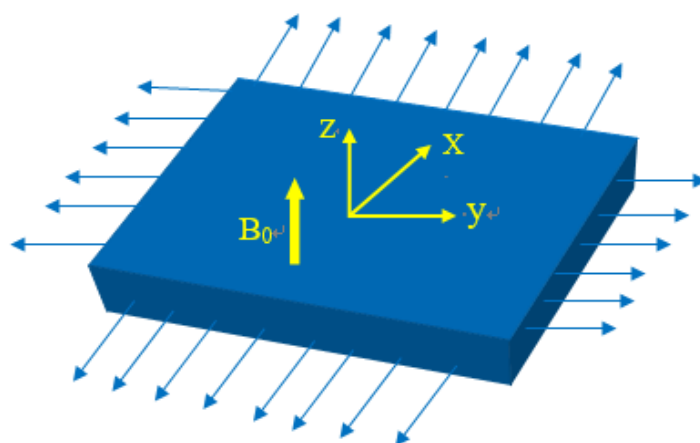


Fig. 1. Flow geometry of the problem

Considering the aforementioned assumptions, the steady boundary layer governing equations indicating conservation of mass, momentum and energy are:

$$\frac{\partial u}{\partial x} + \frac{\partial v}{\partial y} + \frac{\partial w}{\partial z} = 0 \quad (1)$$

$$u \frac{\partial u}{\partial x} + v \frac{\partial u}{\partial y} + w \frac{\partial u}{\partial z} = \frac{\mu_{nf}}{\rho_{nf}} \frac{\partial^2 u}{\partial z^2} - \frac{\sigma_{nf} B^2 u}{\rho_{nf}} \quad (2)$$

$$u \frac{\partial v}{\partial x} + v \frac{\partial v}{\partial y} + w \frac{\partial v}{\partial z} = \frac{\mu_{nf}}{\rho_{nf}} \frac{\partial^2 v}{\partial z^2} - \frac{\sigma_{nf} B^2 v}{\rho_{nf}} \quad (3)$$

$$u \frac{\partial T}{\partial x} + v \frac{\partial T}{\partial y} + w \frac{\partial T}{\partial z} = \frac{k_{nf}}{(\rho C_p)_{nf}} \frac{\partial^2 T}{\partial z^2} + \frac{16\sigma^* T_\infty^3}{3k^* (\rho C_p)_{nf}} \frac{\partial^2 T}{\partial z^2} \quad (4)$$

$$\text{where } \sigma_{nf} = \sigma_f \left[1 + \frac{3 \left(\frac{\sigma_p}{\sigma_f} - 1 \right) \phi}{\left(\frac{\sigma_p}{\sigma_f} + 2 \right) - \left(\frac{\sigma_p}{\sigma_f} - 1 \right) \phi} \right]$$

In the energy equation (4), the term $\frac{16\sigma^* T_\infty^3}{3k^* (\rho C_p)_f} \frac{\partial^2 T}{\partial z^2}$ is obtained by assuming the temperature variation within the flow as small and expanding T^4 in a Taylor series about T_∞ and ignoring higher order terms and using the resulting expression in the Rosseland radiative heat flux [23] $q_r = -\frac{4\sigma^*}{3k^*} \frac{\partial T^4}{\partial z}$.

The boundary conditions read:

$$\left. \begin{aligned} u = U_w = U_0 \exp\left[\frac{x+y}{L}\right], v = V_w = V_0 \exp\left[\frac{x+y}{L}\right], w = 0, -k_f \frac{\partial T}{\partial z} = h_f (T_f - T), \text{ at } z = 0 \\ u \rightarrow 0, v \rightarrow 0, T \rightarrow T_\infty, \text{ as } z \rightarrow \infty \end{aligned} \right\} \quad (5)$$

where u , v and w are velocity components along the x , y and z -directions, respectively, ν_f is the kinematic viscosity, T_∞ is the free stream temperature, σ is the electrical conductivity, B_0 is the maximum strength of variable magnetic field, ρ_f is the fluid density, U_0, V_0, U_w and V_w are constant velocities, L is the reference length, k_f is the thermal conductivity, h_f is the convective heat transfer coefficient, T_f is the temperature of the fluid heating the surface of the sheet, σ^* and k^* are respectively the Stefan-Boltzmann constant, and mean absorption coefficient. The effective density of the nanofluid ρ_{nf} and the heat capacitance of the nanofluids $(\rho C_p)_{nf}$ are defined in [24-26] as

$$\left. \begin{aligned} \rho_{nf} &= (1-\phi)\rho_f + \phi\rho_s \\ (\rho C_p)_{nf} &= (1-\phi)(\rho C_p)_f + \phi(\rho C_p)_s \end{aligned} \right\} \quad (6)$$

where $(\rho C_p)_f$ and $(\rho C_p)_s$ are respectively the heat capacitances of the base fluid and the nanoparticles, ρ_s and ρ_f are the densities of the pure fluid and the nanoparticles, respectively.

The effective dynamic viscosity of the nanofluid is described in [24-26] as

$$\mu_{nf} = \mu_f (1 + 39.11\phi + 533.9\phi^2) \quad (7)$$

where μ_{nf} and μ_f are the effective dynamic viscosities of the nanofluid and the base fluid respectively, and ϕ is the solid volume fraction of nanoparticles.

Following the micro-convection model proposed by Patel et al. [22], the effective thermal conductivity of the nanofluid can be determined as

$$\left. \begin{aligned} \frac{k_{nf}}{k_f} &= 1 + \frac{k_s A_s}{k_f A_f} + c k_s P_e \frac{A_s}{k_f A_f} \\ \frac{A_s}{A_f} &= \frac{d_f}{d_s} \frac{\phi}{1-\phi} \\ P_e &= \frac{u_s d_s}{\alpha_f}, u_s = \frac{2k_B T}{\pi \mu_f d_s^2}, c = 25,000 \end{aligned} \right\} \quad (8)$$

where k_{nf} , k_f and k_s are respectively the thermal conductivities of the nanofluid, base fluid and the nanoparticles, A_s and A_f are the heat transfer area corresponding to particles and fluid media, respectively, $c(>0)$ is a constant, Pe is the Peclet number, d_f is the molecular size of the fluid and d_s is the nanoparticle diameter, u_s is the Brownian motion velocity, α_f is the thermal diffusivity of the fluid, and μ_f is the dynamic viscosity of the fluid.

In order to facilitate the analysis, we need the transformations:

$$\left. \begin{aligned} u &= U_0 \exp\left[\frac{x+y}{L}\right] F'(\eta), v = U_0 \exp\left[\frac{x+y}{L}\right] G'(\eta), \\ w &= -\sqrt{\frac{\nu_f U_0}{2L}} \exp\left[\frac{x+y}{2L}\right] [F(\eta) + \eta F'(\eta) + G(\eta) + \eta G'(\eta)], \\ \theta(\eta) &= \frac{T - T_\infty}{T_f - T_\infty}, \\ \eta &= \sqrt{\frac{U_0}{2\nu_f L}} \exp\left[\frac{x+y}{2L}\right] z \end{aligned} \right\} \quad (9)$$

Using Eq. (9), Eqs. (2-5) read

$$\phi_1 F''' + (F + G)F'' - 2(F' + G')F' - \phi_2 MF' = 0 \quad (10)$$

$$\phi_1 G''' + (F + G)G'' - 2(F' + G')G' - \phi_2 MG' = 0 \quad (11)$$

$$\frac{1}{\text{Pr}} \left(\phi_3 + \frac{4}{3} \phi_4 R_d \right) \theta'' + (F + G)\theta' = 0 \quad (12)$$

$$\left. \begin{aligned} F = 0, G = 0, F' = 1, G' = \beta, \theta'(0) = -B_i [1 - \theta(0)] \text{ at } \eta = 0 \\ F' \rightarrow 0, G' \rightarrow 0, \theta \rightarrow 0 \quad \text{as } \eta \rightarrow \infty \end{aligned} \right\} \quad (13)$$

where

$$\left. \begin{aligned} M = \frac{2\sigma B_0^2 L}{\rho_f U_0}, \beta = \frac{V_0}{U_0}, P_r = \frac{\nu_f}{\alpha_f}, R_d = \frac{4\sigma^* T_\infty^3}{3k_f k^*}, \\ Bi = \frac{\varepsilon}{k_f \sqrt{\frac{U_0}{2\nu_f L}}}, \varepsilon = \frac{h_f}{\exp\left(\frac{x+y}{2L}\right)} \end{aligned} \right\} \quad (14)$$

Here M, β, Pr, R_d and Bi are respectively being the Hartmann number, ratio parameter, Prandtl number, thermal radiation parameter and Biot's number. The nanoparticle volume fraction constants $\phi_i (i = 1, 2, 3, 4)$ are defined as

$$\phi_1 = \frac{\nu_{nf}}{\nu_f} = \frac{1 + 39.11\phi + 533.9\phi^2}{1 - \phi + \phi(\rho_s / \rho_f)}, \phi_2 = \frac{\rho_f}{\rho_{nf}} = \frac{1}{1 - \phi + \phi(\rho_s / \rho_f)},$$

$$\phi_3 = \frac{1 + \frac{k_s}{k_f} \frac{d_f}{d_s} \left(\frac{\phi}{1 - \phi} \right) + c \frac{k_s}{k_f} Pe \left(\frac{\phi}{1 - \phi} \right)}{1 - \phi + \phi[(\rho C_p)_s / (\rho C_p)_f]}, \phi_4 = \frac{1}{1 - \phi + \phi[(\rho C_p)_s / (\rho C_p)_f]},$$

The skin friction coefficients along axial and transverse directions are:

$$C_{fx} = \frac{\tau_{wx}}{\left(\frac{1}{2}\right) \rho_f U_w^2} \quad (15)$$

$$C_{fy} = \frac{\tau_{wy}}{\left(\frac{1}{2}\right) \rho_f V_w^2} \quad (16)$$

where τ_{wx} and τ_{wy} are the wall shear stresses.

The dimensionless form of the skin friction coefficient along axial and transverse directions are obtained respectively as

$$\left(\frac{\text{Re}_x}{2}\right)^{\frac{1}{2}} C_{fx} = (1 + 39.11\phi + 533.9\phi^2) F''(0) \quad (17)$$

$$\left(\frac{\text{Re}_y}{2}\right)^{\frac{1}{2}} C_{fy} = (1 + 39.11\phi + 533.9\phi^2) G''(0) \quad (18)$$

The local Nusselt number,

$$Nu_x = \frac{xq_w}{k_f(T_w - T_\infty)} \quad (19)$$

where q_w is the wall heat flux.

The dimensionless local Nusselt number is

$$\left(\frac{\text{Re}_x}{2}\right)^{-\frac{1}{2}} Nu_x = -\left(\frac{k_{nf}}{k_f} + Rd\right) \frac{x}{L} \theta'(0) \quad (20)$$

Where $\text{Re}_x = \frac{U_w L}{\nu_f}$ and $\text{Re}_y = \frac{V_w L}{\nu_f}$ are the local Reynolds numbers.

3. Results and Discussion

The influence of variable magnetic field and thermal radiation on three-dimensional nanofluid flows past an exponentially-stretching sheet has been investigated in the present study. In addition, the Patel model [22] is applied for an appreciable enhancement of the thermal conductivity and hence, the heat transfer capability of nanofluids. Furthermore, a convective heat transfer model is employed where the bottom surface of the plate gets heated from a hot fluid of temperature T_j providing a heat transfer coefficient h_j . The fourth-order Runge-Kutta method is employed to obtain the solutions of the transformed governing boundary layer equations along with the transformed boundary conditions. In the present analysis, we consider three different kinds of base fluids such as water, water with 30% ethylene glycol, water with 50% ethylene glycol. It is inevitable to declare that three nanoparticles such as Cu (copper), Ag (silver) and Al_2O_3 (alumina) have been chosen in the present study. The general and thermal properties of both the base fluids and the nanoparticles are incorporated in Table 1. To get the accuracy, the

results obtained and presented in the present study are compared and validated in Table 2 with the noteworthy works of Nadeem et al. [13], Magyari and Keller [27] and Liu et al. [28]. These comparisons as well as the validation confirm that our numerical results are found to be agreed well for all considered values of parameters and therefore, we are confident about the accuracy and generality of our results.

The impact of the pertinent parameters on the dimensionless velocity, temperature, skin friction and the Nusselt number is demonstrated through Figs. 2–16 and Table 3. To begin with Figs. 2 and 3 portray the developed variation of the velocity profiles along the axial and transverse directions for different values of the Hartmann number M . The figures display, in rich detail, the fact that both the axial and transverse velocities attain deceleration with the enhancement of the Hartmann number associated with a thinner momentum boundary layer. This is obvious due to the reason that the electromagnetic interaction between the magnetic field and electrically-conducting fluid establish a retarding Lorentz force that impedes the fluid motion in the entire boundary layer region. The most fascinating aspect of this observation is that the deceleration of velocity is significant for relatively higher values of the Hartmann number. This result is in good agreement with the results in [21].

Fig. 4 confirms the sighting of the non-dimensional temperature profiles under the influence of the Hartmann number M . The important outcome has been accomplished from this sighting is that a higher value of M enables the non-dimensional temperature to rise as is observed earlier in [13]. The only basic reason for this enhancement is that an increase in the Hartmann number generates electromagnetic force in greater strength that restrains the fluid motion which in turn causes the temperature rise leading to a thicker thermal boundary layer. In fact, had there been no magnetic field, the temperature could not be enhanced in the flow field. An interesting consequence of the temperature profiles due to the presence of magnetic field is that the rise in the fluid temperature is significant for relatively higher values of the Hartmann number M .

Before we go further and study the influence of the Prandtl number Pr on the non-dimensional temperature, it is necessary to understand the meaning of Prandtl number. Physically, the Prandtl number is nothing but the ratio of the kinematic viscosity to the thermal diffusivity. We express this influence by saying that a higher Prandtl fluid such as ethylene glycol (30% with $Pr = 13.5$ and 50% with $Pr = 24.4$) having a lower thermal diffusivity (lower thermal conductivity) reduces conduction and thereby decreasing the thermal resistance (causes a reduction in the fluid temperature) in association with the thermal boundary layer shrinks whereas the reverse effect is attained for a lower Prandtl fluid such as water ($Pr = 7$) as illustrated

in Fig.5. In other words, an increase in the Prandtl number enhances the heat transfer rate at the surface as the temperature gradient at the surface gets enhanced [17].

A significant impact of radiation effect on the non-dimensional temperature is displayed in Fig.6. It focuses that the non-dimensional fluid temperature increases due to an increase in the radiation parameter leading to a growth of the thermal boundary layer. Hence, it is always advisable to keep the thermal radiation to a minimum so as to accomplish more heat transfer rate and thereby, producing more cooling [20].

The characteristics of the axial and transverse velocities as well as the temperature profiles for different nanoparticles volume fraction ϕ are revealed from Figs.7 – 9. From these illustrations, it follows that the axial as well as the transverse velocities get enhanced in association with the growing momentum boundary layer due to an increase in ϕ while the opposite trend prevails for the fluid temperature indicating a decrease in the thermal resistance under the influence of this pertinent parameter that causes narrowing of the thermal boundary layer [21].

It is found from Fig.10 that the non-dimensional temperature and hence, the thermal resistance increases due to an enhancement in the Biot number Bi . However, the increase is significant for higher Bi values. The variations of the non-dimensional velocities (axial as well as transverse) and the non-dimensional temperature of the fluid in response to different values of the stretching ratio are made known from Figs.11-13. Actually, the stretching ratio is the ratio between the transverse and axial velocities of the stretching sheet. An increase in the stretching ratio means that the transverse velocity becomes larger than the axial velocity. Considering the above concept in mind and observing from the Figs.11 and 12 that the axial velocity decreases due to an increase in the stretching ratio parameter β while the transverse velocity shows the opposite trend. However, it must be noted from Fig.13 that the non-dimensional temperature and hence, the thermal resistance of the fluid decreases due to an increase in the stretching ratio parameter thereby shrinking the thermal boundary layer thickness [29].

Figs.14 and 15 disclose the behavior of the axial as well as the transverse skin friction with the nanoparticles volume fraction for different Hartmann number M . It is well understood from this figure that the axial as well as the transverse skin friction reduce due to an increase in the value of M for pure water as the base fluid with Cu nanoparticles. In other words, an increase in the magnetic field strength causes reduction in the axial as well as the transverse wall shear stresses in the entire flow domain.

The variation of the reduced Nusselt number $-\theta'(0)$ with the increase in the Hartmann

number M affiliated with the nanoparticles volume fraction is seen in Fig. 16. One must acknowledge here that the increase in the magnetic field strength enhances the thermal resistance thereby enhancing the fluid temperature which in turn reduces the heat transfer rate from the surface indicating less cooling.

Table 2 provides comparisons of the present results with the results published earlier by noteworthy researchers like Nadeem et al. [13], Magyari and Keller [27] and Liu et al. [28] available in the literature. In these comparisons, we find that an increase in the Prandtl number Pr for a pure fluid decreases the thermal resistance thereby increasing the heat transfer rate. This result is well-agreed with Nadeem et al. [13], Magyari and Keller [27] and Liu et al. [28].

From the data incorporated in Table 3, it is obvious that an increase in the Hartmann number M decreases the axial as well as the transverse skin frictions for all nanoparticles such as Ag, Cu and Al_2O_3 . However, at a fixed value of M , the axial and transverse skin frictions (absolute values) increase in the order of choice of nanoparticles viz. Ag, Cu and Al_2O_3 . We say that an increase in the Hartmann number M disparages the heat transfer rate. There is a good, valid and compelling reason for such diminution of the local skin frictions as well as hike of the wall temperature gradient that the retarding Lorentz force restrains the fluid motion from its pristine condition and boosts the strength of the thermal resistance thereby enhancing the non-dimensional fluid temperature. Another point to be noted is that at fixed value of M , the heat transfer rate gets enhanced in the order of nanoparticles Ag, Cu and Al_2O_3 indicating more cooling from the surface.

It is pertinent that an increase in the thermal radiation enhances the heat transfer rate from the surface for all nanoparticles viz. Ag, Cu and Al_2O_3 . Notwithstanding, the nanoparticles types like Ag, Cu and Al_2O_3 , an increase in the ratio parameter β decreases the axial as well as the transverse wall shear stresses whereas the influence of β attains a reverse trend on the heat transfer rate. One can say that there is an increase in the wall temperature gradient due to the Biot number Bi for all nanoparticles. Let us discuss in a little more detail the impact of nanoparticles volume fraction ϕ on the local skin frictions and the rate of heat transfer. It has been traced that the axial as well as the transverse skin frictions (or wall shear stresses) and the heat transfer rate get enhanced due to an increase in the value of ϕ .

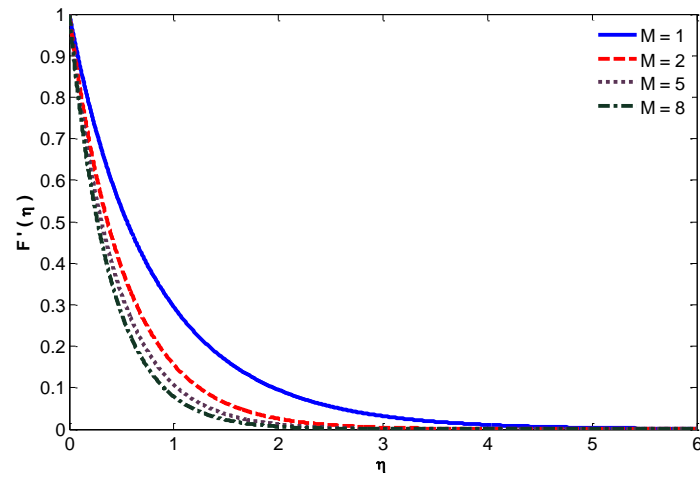


Fig.2. Axial velocity profile for different Hartman number (pure water, Cu nanoparticles)

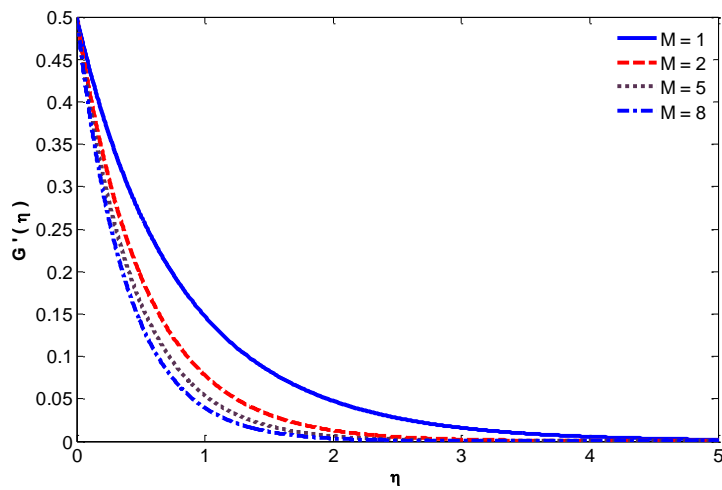


Fig. 3. Transverse velocity profile for different Hartman number (pure water, Cu nanoparticles)

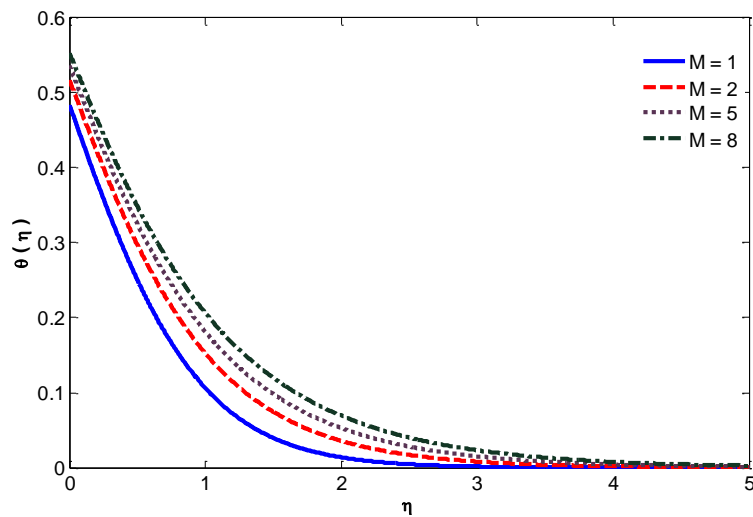


Fig.4. Temperature profile for different Hartman number (pure water, Cu nanoparticles)

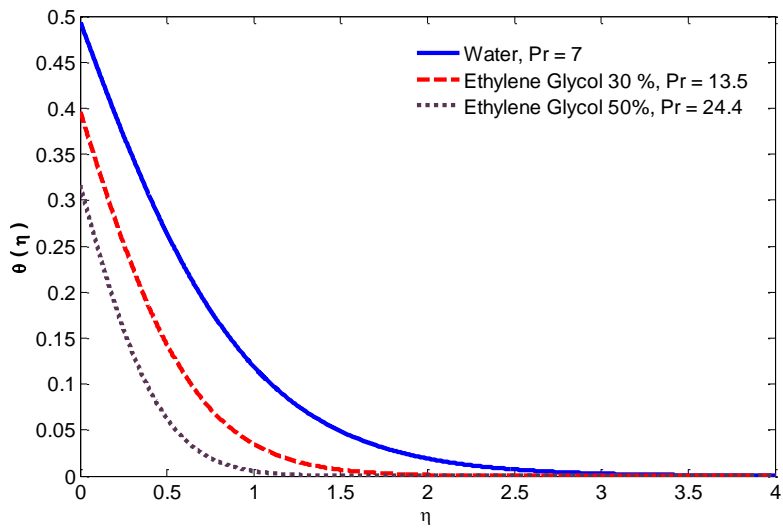


Fig. 5. Temperature profile for different Prandtl number (Cu nanoparticles)

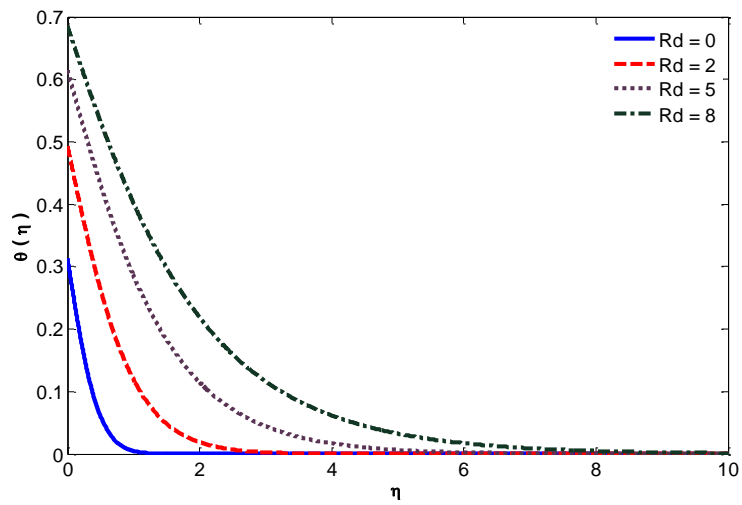


Fig. 6. Temperature profile for different radiation parameter (Cu nanoparticles)

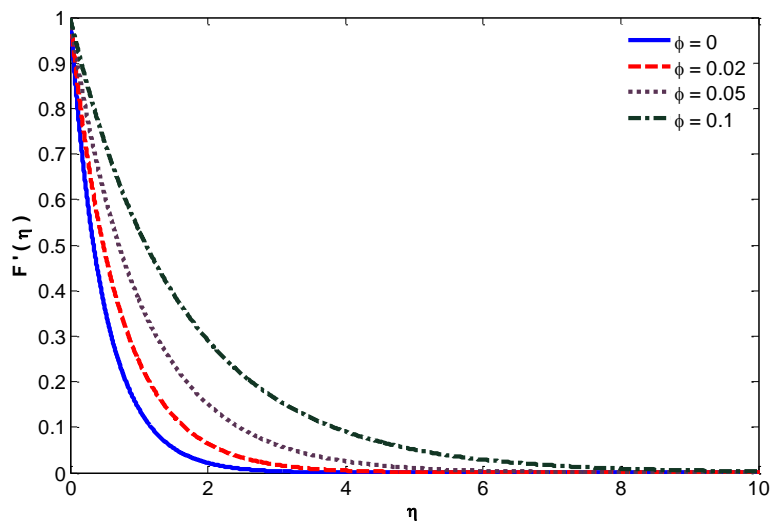


Fig. 7. Axial velocity for different volume fraction (pure water, Cu nanoparticles)

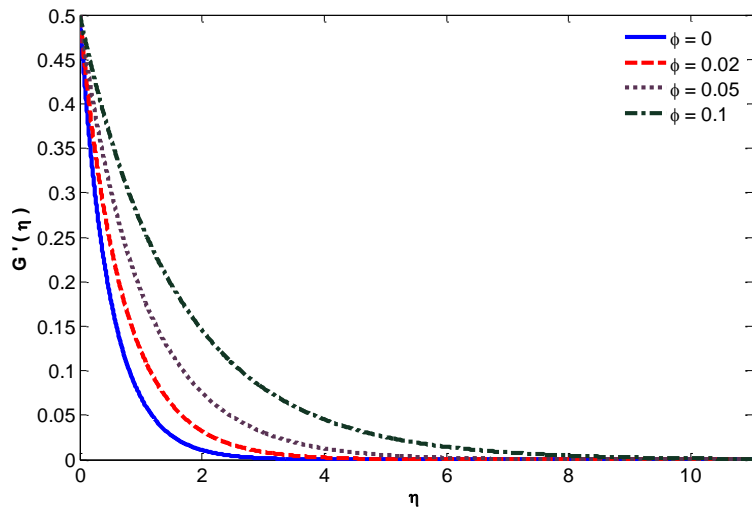


Fig. 8. Transverse velocity for different volume fraction (pure water, Cu nanoparticles)

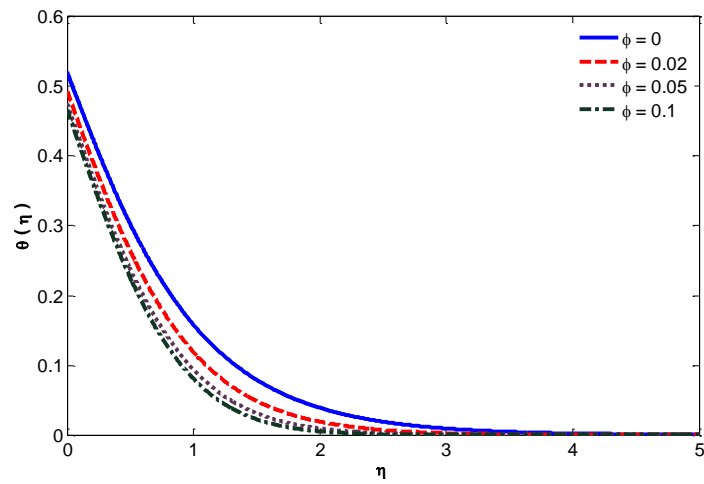


Fig. 9. Temperature profile for different volume fraction (pure water, Cu nanoparticles)

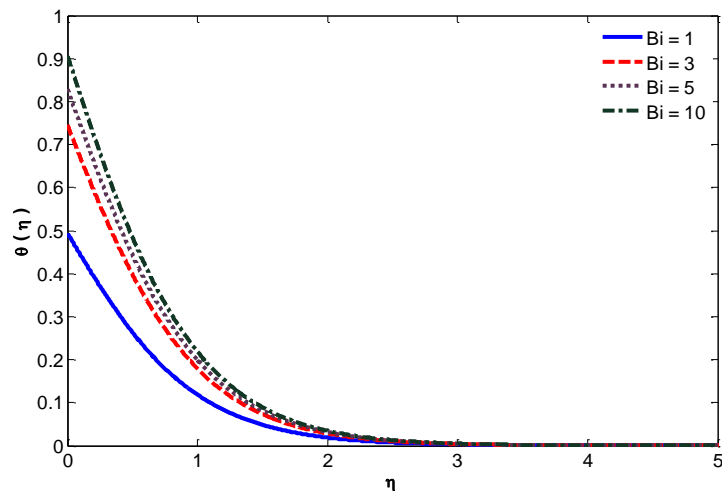


Fig.10. Temperature profile for different Biot number (pure water, Cu nanoparticles)

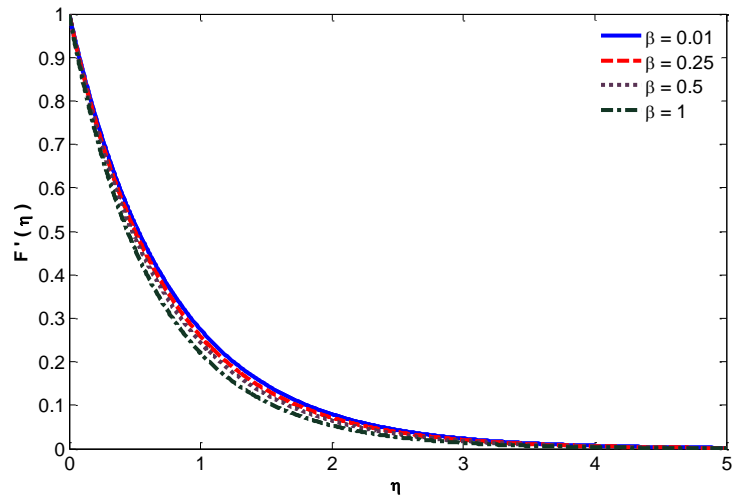


Fig.11. Axial velocity profile for different ratio parameter (pure water, Cu nanoparticles)

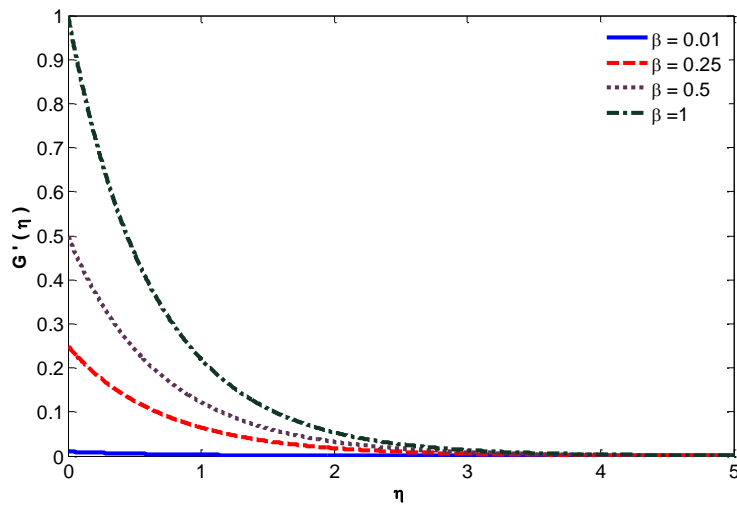


Fig.12. Transverse velocity profile for different ratio parameter (pure water, Cu nanoparticles)

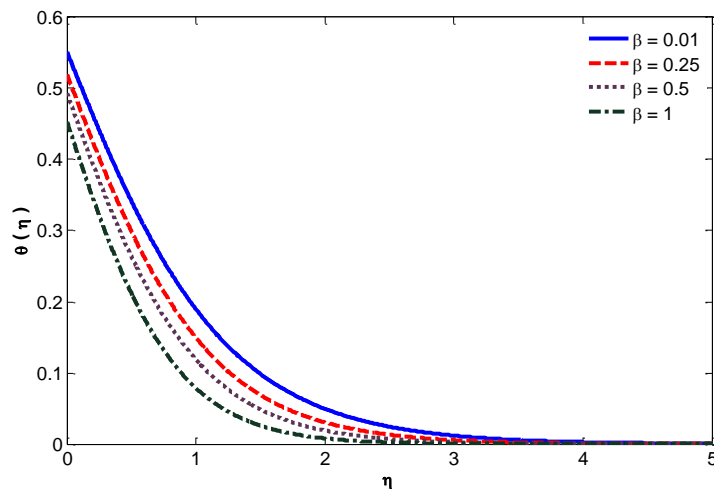


Fig.13. Temperature profile for different ratio parameter (pure water, Cu nanoparticles)

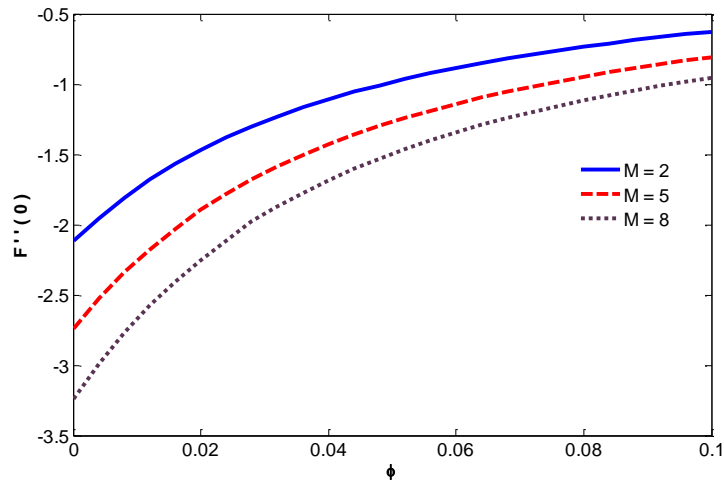


Fig. 14. Axial skin friction in response to volume fraction for different Hartman number (pure water, Cu nanoparticles)

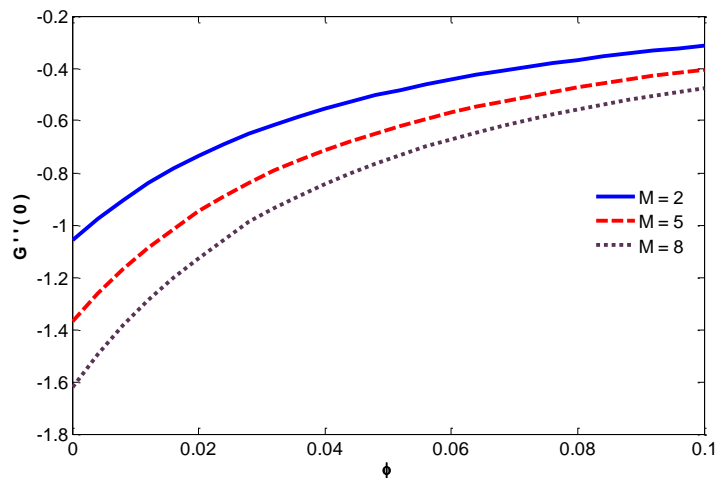


Fig. 15. Transverse skin friction in response to volume fraction for different Hartman number (pure water, Cu nanoparticles)

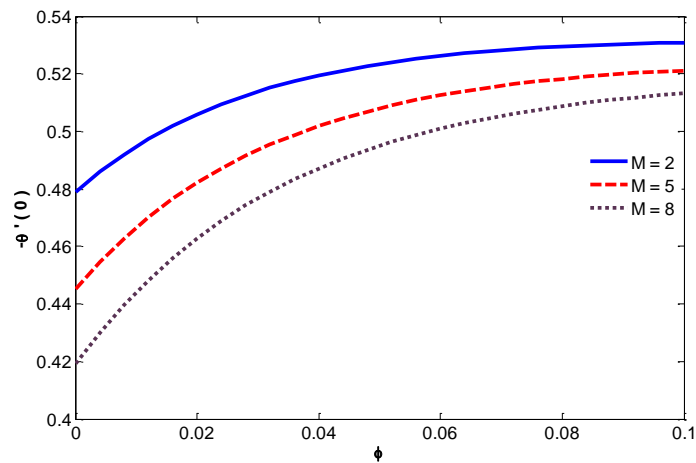


Fig. 16. Local Nusselt number in response to volume fraction for different magnetic parameter (pure water, Cu nanoparticles)

Tab 1. Thermo-physical properties of the base fluid and nanoparticles at T=300K.

	ρ (Kg/m ³)	C_p (J/Kg K)	k (W/m K)	μ_f (N s/m ²)	d_f or d_s (nm)
Pure Water	997.1	4179	0.613	0.001003	0.24
Ethylene glycol 30%	1034	3736.2	0.489	0.0017613	0.45
Ethylene glycol 50%	1052.1	3301.7	0.432		30-60
Copper (Cu)	8933	385	401		30-60
Silver (Ag)	10500	2235	429		30-60
Alumina (Al ₂ O ₃)	3970	765	40		30-60

Tab 2. Comparison with the literature of heat transfer rate for pure fluid M=0, A=0, $\beta = 0$ results with Magyari and Keller [27], Liu et al. [28], Nadeem et al. [13].

Pr	Magyari and Keller[27]	Liu et al. [28]	Nadeem et al. [13]	Present
0.7		-0.4258380	-0.42584	-0.42583456
1	-0.549643	-0.54964375	- 0.549646	-0.54964072
5	-1.521243	-1.52123900	-1.521240	-1.52121586
7		-1.8466056	-1.84661	
10	-2.257429	-2.25742372	-2.257424	--2.25737274

Tab 3. Skin frictions $F''(0)$ and $G''(0)$ and local Nusselt number $-\theta'(0)$ for different $\phi, A, \beta, \lambda_T, M, Bi$ with Pr = 7.

ϕ	Bi	β	Rd	M	$F''(0)$	$G''(0)$	$-\theta'(0)$
0.02	1	0.5	2	2	-1.49379940 (Cu)	-0.74689970 (Cu)	0.50598557 (Cu)
					-1.49696035 (Al ₂ O ₃)	-0.74848018 (Al ₂ O ₃)	0.50814768 (Al ₂ O ₃)
					-1.49254979 (Ag)	-0.74627490 (Ag)	0.50508328 (Ag)
	10				-1.49379940 (Cu)	-0.74689970 (Cu)	0.92907363 (Cu)
					-1.49696035 (Al ₂ O ₃)	-0.74848018 (Al ₂ O ₃)	0.93638936 (Al ₂ O ₃)
					-1.49254979 (Ag)	-0.74627490 (Ag)	0.92603608 (Ag)
	1	0.75			-1.56062742 (Cu)	-1.17047057 (Cu)	0.52781722 (Cu)
					-1.56415506 (Al ₂ O ₃)	-1.17311629 (Al ₂ O ₃)	0.52994638 (Al ₂ O ₃)
					-1.55923271 (Ag)	-1.16942453 (Ag)	0.52692839 (Ag)
		0.5	5		-1.49379940 (Cu)	-0.74689970 (Cu)	0.38444316 (Cu)
					-1.49696035 (Al ₂ O ₃)	-0.74848018 (Al ₂ O ₃)	0.38524039 (Al ₂ O ₃)
					-1.49254979 (Ag)	-0.74627490 (Ag)	0.38362390 (Ag)
			2	5	-1.93342640 (Cu)	-0.96671320 (Cu)	0.48225584 (Cu)

					-1.93587858 (Al ₂ O ₃)	-0.96793929 (Al ₂ O ₃)	0.48463949 (Al ₂ O ₃)
					-0.77725136 (Ag)	-0.35353036 (Ag)	1.46714265 (Ag)
0.05				2	-1.01360975 (Cu)	-0.50680487 (Cu)	0.52388398 (Cu)
					-1.01901889 (Al ₂ O ₃)	-0.50950944 (Al ₂ O ₃)	0.52903285 (Al ₂ O ₃)
					-1.01146649 (Ag)	-0.50573325 (Ag)	0.52175609 (Ag)

4. Conclusion

The effects of a variable magnetic field as well as thermal radiation associated with the pertinent governing parameters on the flow of an electrically-conducting incompressible nanofluid over an exponentially-stretching sheet in response to a convective boundary condition have been discussed with the help of graphs and tables. In the present study, Patel model [22] is employed so as to enhance the thermal conductivity and hence the heat transfer capability of nanofluids. The obtained numerical results are in conformity with the previous results published by Nadeem et al. [13], Magyari and Keller [27] and Liu et al. [28]. The major concluding remarks of the present study are:

1. The electromagnetic interaction between the magnetic field and the electrically-conducting fluid develops a restraining Lorentz force that impedes the fluid motion along the axial as well as the transverse directions and enhances the thermal resistance leading to a thinner velocity boundary layer and a thicker thermal boundary layer in the entire boundary layer region.
2. The axial as well as the transverse velocities get reduced due to an increase in in the value of β while those velocities attain a reverse trend due to an increase in in the value of ϕ .
3. The Prandtl number Pr proves to be most effective in influencing the thermal resistance and hence, the non-dimensional fluid temperature in a descending trend offering a significant heat transfer rate wherein the thermal boundary layer shrinks.
4. An increase in the Biot number enhances the heat transfer rate while an increase in the thermal radiation exhibits the reverse trend on the rate of heat transfer. Therefore, thermal radiation is to be kept minimum so as to accomplish more cooling from the concerned system.
5. The wall shear stresses (axial as well as transverse) and the heat transfer rate follow a descending trend due to increases in the magnetic field strength in the entire flow domain for all types of nanoparticles viz. Ag , Cu and Al_2O_3 and for a pure fluid.

References

1. S.U.S. Choi, Enhancing thermal conductivity of fluids with nanoparticles, 1995, ASME

- Fluids Eng. Division, vol. 231, pp. 99–105.
2. W. Khan and I. Pop, Boundary-layer flow of a nanofluid past a stretching sheet, 2010, *Int. J. Heat Mass Transfer*, vol. 53, pp. 2477-2483.
 3. O. Makinde, A. Aziz, Boundary layer flow of a nanofluid past a stretching sheet with a convective boundary condition, 2011, *Int. J. Ther. Sci.*, vol. 50, pp. 1326-1332.
 4. M. Sheikholeslami, S.A. Shehzad, Thermal radiation of ferrofluid in existence of Lorentz forces considering variable viscosity, 2017, *Int. J Heat Mass Transf.*, vol. 109, pp. 82–92.
 5. F.A.B. Aamina, I. Khan, A. Nadeem, S.M. Saqib Magnetohydrodynamic flow of brinkman-type engine oil based MoS₂-nanofluid in a rotating disk with hall effect, *Int. J Heat Technology*.
 6. A.K. Pandey, M. Kumar, Natural convection and thermal radiation influence on nanofluid flow over a stretching cylinder in a porous medium with viscous dissipation, 2017, *Alexandria Eng. J.*, vol. 56, pp. 55–62.
 7. A. Alsabery, A.J. Chamkha and I. Hashim, Heat line visualization of conjugate natural convection in a square cavity filled with nanofluid with sinusoidal temperature variations on both horizontal walls, 2016, *Int. J. Heat Mass Transf.*, vol. 100, pp. 835-850.
 8. S. Reddy, A. J. Chamkha, Soret and Dufour effects on MHD convective flow of Al₂O₃-water and TiO₂-water nanofluids past a stretching sheet in porous media with heat generation/absorption, 2016, *Adv. Powder Technol.*, vol. 27, pp. 1207-1218.
 9. M.K. Nayak, G.C. Dash, L.P. Singh, Unsteady radiative MHD free convective flow and mass transfer of a viscoelastic fluid past an inclined porous plate, 2015, *Arab. J. Sci. Eng.*, vol. 40, pp. 3029-3039.
 10. M. K. Nayak, G. C. Dash, L. P. Singh, Steady MHD flow and heat transfer of a third grade fluid in wire coating analysis with temperature dependent viscosity, 2014, *Int. J. Heat Mass Transf.*, vol. 79, pp. 1087–1095.
 11. M. Sheikholeslami, M. Hatami, D.D. Ganji, Nanofluid flow and heat transfer in a rotating system in the presence of a magnetic field, 2014, *J. Mol. Liq.*, vol. 190, pp. 112-120.
 12. M.A. Ismael, M.A. Mansour, A.J. Chamkha, A.M. Rashad, Mixed convection in a nanofluid filled-cavity with partial slip subjected to constant heat flux and inclined magnetic field, 2016, *J. Magn. Mater.*, vol. 416, pp. 25–36.
 13. S. Nadeem, R. U. Haq, Z.H. Khan, Heat transfer analysis of water-based nanofluid over an exponentially stretching sheet, 2014, *Alex. Eng. J.*, vol. 53, no. 1, pp. 219–224.
 14. T. Hayat, M. Shafique, A. Tanveer, A. Alsaedi, Magnetohydrodynamic effects on peristaltic flow of hyperbolic tangent nanofluid with slip conditions and Joule heating in an inclined

- channel, 2016, *Int. J. Heat Mass Transf.*, vol. 102, pp. 54–63.
15. O.D. Makinde, I.L. Animasaun, Bioconvection in MHD nanofluid flow with nonlinear thermal radiation and quartic autocatalysis chemical reaction past an upper surface of a paraboloid of revolution, 2016, *Int. J. Ther. Sci.*, vol. 109, pp. 159-171.
 16. A. Aziz, A similarity solution for laminar thermal boundary layer over a flat plate with a convective surface boundary condition, 2009, *Comm. Nonlinear Sci. Num. Simul.*, vol. 14, no. 4, pp. 1064-1068.
 17. M.K. Nayak, MHD 3D flow and heat transfer analysis of nanofluid by shrinking surface inspired by thermal radiation and viscous dissipation, 2017, *Int. J. Mech. Sci.*, vol. 124-125, pp. 185-193.
 18. Nayak DT [tsep].
 19. O.D. Makinde, A. Ogulu, The effect of thermal radiation on the heat and mass transfer flow of a variable viscosity fluid past a vertical porous plate permeated by a transverse magnetic field, 2008, *Chem. Eng. Commn.*, vol. 195, no. 12, pp. 1575–1584.
 20. M.K. Nayak, Chemical reaction effect on MHD viscoelastic fluid over a stretching sheet through porous medium, 2016, *Meccanica*, vol. 51, pp. 1699-1711.
 21. F. Mabood, S. Shateyi, M.M. Rashidi, E. Momoniat, N. Freidoonimehr, MHD stagnation point flow heat and mass transfer of nanofluids in porous medium with radiation, viscous dissipation and chemical reaction, 2016, *Adv. Powder Technol.*, vol. 27, pp. 742-749.
 22. H.E. Patel, T. Sundararajn, T. Pradeep, A. Dasgupta, N. Dasgupta and S.K. Das, A micro-convection model for thermal conductivity of nanofluids, 2005, *Pramana J. Physics*, vol. 65, no. 5, pp. 863-869.
 23. M. Q. Brewster, *Thermal radiative transfer properties*, 1972, Wiley, New York.
 24. B.C. Pak, Y.I. Cho, Hydromagnetic and heat transfer study of dispersed fluids with submicron metallic oxide particles, 1998, *Exp. Heat Transfer*, vol. 11, pp. 151-171.
 25. M.K. Nayak, N.S. Akbar, V.S. Pandey, Z.H. Khan, D. Tripathi, 3D free convective MHD flow of nanofluid over permeable linear stretching sheet with thermal radiation, 2017, *Powder Technol.*, vol. 315, pp. 205-215.
 26. O. Pourmehran, M. Rahimi-Gorji, D.D. Ganji, heat transfer and flow analysis of nanofluid flow induced by a stretching sheet in the presence of an external magnetic field, 2016, *J. Taiwan Inst. Chem. Eng.*, vol. 65, pp. 162-171.
 27. E. Magyari, B. Keller, Heat and mass transfer in the boundarylayers on an exponentially stretching continuous surface, 1999, *J. Phy. D. Appl. Phy.*, vol. 32, pp. 577–585.
 28. C. Liu, Hung-H.Wang, Yih-F.Peng, Flow and heat transfer forthree-dimensional flow over an

- exponentially stretching surface, 2013, *Chemical Eng. Com.*, vol. 200, pp. 253–268.
29. W. Ibrahim, B. Shankar, M.M. Nandeppanavar, MHD stagnation point flow and heat transfer due to nanofluid towards a stretching sheet, 2013, *Int. J. Heat Mass Transf.*, vol. 56, pp. 1-9.